

PREDICTION OF MASS TRANSFER COLUMNS WITH DUMPED AND ARRANGED PACKINGS

Updated Summary of the Calculation Method of Billet and Schultes

R. BILLET and M. SCHULTES*

Ruhr-University Bochum, Bochum, Germany
*Raschig GmbH, Ludwigshafen, Germany

A good knowledge of the relationship between the two-phase countercurrent flow of a packed mass transfer column is essential for the design of rectification, absorption and desorption columns. Based on a physical model the authors describe their updated equations for calculating gas and liquid side mass transfer coefficients, pressure drop of dry or irrigated random and structured packings, their loading and flooding points as well as their liquid holdup. Based on one of the largest experimental databases in the world, the calculated results give only small deviations from the database

Keywords: packings; mass transfer; mass transfer coefficients; pressure drop; loading point; flooding point; liquid holdup

INTRODUCTION

Until a few years ago, mass transfer columns with dumped or arranged packings were designed on the basis of empirical calculation approaches which, although they were based on experimental data, could not be traced back to any physical context. These relations always resulted in unproven designs when applied outside of the experimental database.

Modern calculation approaches are based, therefore, on physically proven conditions of fluid dynamics in mass transfer columns and take into account the kinetic laws of mass transfer in flowing media. The calculation model by Billet and Schultes is such a physically proven model for the advanced calculation of mass transfer columns with dumped or arranged packings. It makes it possible to determine the mass transfer efficiency, the pressure drop, the column holdup and the load limits on the basis of a uniform theory. The results of this calculation method agree well with one of the largest experimental database for results of investigation on mass transfer columns. This database was compiled under the supervision of Prof Dr-Ing R. Billet of the Ruhr-Universität Bochum and includes over 3500 measured data, more than 50 test systems and is based on measurements with over 70 types of dumped and arranged packings, see Table 1.

The basis of this calculation approach is a model which assumes that the empty space of dumped or arranged packings can be replaced for theoretical considerations by vertical flow channels, through which the liquid trickles evenly distributed downwards while the gas flows upwards in the counterflow. In reality, however, the flow channels deviate from the vertical and are decisively determined by the shape of the dumped packings or of the arranged packing. Since the geometrical shape, however, cannot be only defined by the surface area or the void volume, the

model assumes that the deviation of the real flow behaviour of the phases from the vertical flow channels in mass transfer columns can be expressed by a packing-specific shape constant.

CALCULATION OF THE MASS TRANSFER EFFICIENCY

For a given separation task, the height of a mass transfer column is calculated according to the HTU-NTU model. According to this, in the case of systems with predominantly gas-phase mass transfer resistance, the product is formed from the overall height of a gas-phase mass transfer unit HTU_{OV} and the number of gas-phase mass transfer units NTU_{OV} for the calculation of the height H , see equation (1). The number of mass transfer units is defined by the concentrations of the incoming and outgoing flows of material and by the phase equilibrium and is therefore essentially dependent on the separation task and the thermodynamic properties. On the other hand, the height of a mass transfer unit is determined by the actual design of the column and the load of the internals. Therefore, the loading capacity of the dumped or arranged packing determines the column diameter and thus the flow velocity and the residence time of the phases in the mass transfer apparatus.

The geometric surface area of the column packing and its ability to create a turbulent flow of the phases also decides the effectiveness of the mass transfer between the phases.

If the mass transfer resistance is situated mainly in the liquid phase, then the height of the separation column is determined by the product of the overall height of a liquid-phase mass transfer unit HTU_{OL} and the number of liquid-phase mass transfer units NTU_{OL} in accordance with

Table 1. Range of material properties and column loads as well as number of the examined substance systems for the determination of fluid-dynamic and separation variables.

			Loading and flooding point	Column holdup	Pressure drop	Mass transfer
Gas load factor	F_V	$\sqrt{\text{Pa}}$	0.47–4.59	0.10–2.78	0.21–5.09	0.003–2.77
Liquid load	u_L	$\text{m}^3 \text{m}^{-2} \text{h}^{-1}$	4.88–144	1.33–82.8	0.61–60.1	0.256–118
Liquid density	ρ_L	kg m^{-3}	750–1026	800–1810	361–1115	361–1237
Liquid viscosity	ν_L	$\text{m}^2 \text{s}^{-1} \times 10^6$	0.40–104	0.74–142	0.14–99.0	0.14–1.66
Surface tension	σ_L	$\text{kg s}^{-2} \times 10^3$		20.8–86.3		0.7–74.0
Diffusion coefficient	D_L	$\text{m}^2 \text{s}^{-1} \times 10^9$				0.29–6.50
Gas density	ρ_V	kg m^{-3}	0.30–1.37		0.06–28	0.07–97
Gas viscosity	ν_V	$\text{m}^2 \text{s}^{-1} \times 10^6$	8.15–41.5		0.14–106	0.14–126
Diffusion coefficient	D_V	$\text{m}^2 \text{s}^{-1} \times 10^6$				0.29–87.4
Number of systems examined			13	20	25	46

equation (2). The variables of equations (1) and (2) are linked with one another via the stripping factor λ , see equations (3) and (4). The stripping factor is described by the quotient formed by the gradient of the equilibrium curve m_{yx} and the molar phase ratio \dot{L}/\dot{V} .

$$H = HTU_{OV} NTU_{OV} \quad (1)$$

$$H = HTU_{OL} NTU_{OL} \quad (2)$$

$$HTU_{OL} = HTU_{OV} / \lambda \quad (3)$$

$$NTU_{OL} = \lambda NTU_{OV} \quad (4)$$

The following statements apply to systems with predominantly gas-phase mass transfer resistance; the results can, however, be applied also to systems with predominantly liquid-phase mass transfer resistance by means of equation (3).

The overall height of a gas-phase mass transfer unit HTU_{OV} is subdivided into the height of a gas-phase mass transfer unit HTU_V and the height of a liquid-phase mass transfer unit HTU_L , which for their part are defined by the gas- and liquid velocities u_V and u_L with reference to the empty column cross-sections and the volumetric mass transfer coefficients $\beta_V a_{ph}$ and $\beta_L a_{ph}$, see equation (5).

The volumetric mass transfer coefficients are calculated by means of equations (6)–(11) and are dependent on the densities of the phases ρ_V , ρ_L , dynamic viscosities η_V , η_L and the surface tension σ_L , the flow velocities u_V , u_L , the specific surface area a of the packing and the void fraction ε as well as the packing-specific constants C_L and C_V , which can be found in Table 2. The effective liquid velocity \bar{u}_L is calculated from the velocity u_L with reference to the column cross-section and the column holdup h_L .

Furthermore, a_{ph} describes the specific interface area between the phases and d_h the hydraulic diameter of the dumped packings.

$$HTU_{OV} = HTU_V + \lambda HTU_L = \frac{u_V}{\beta_V a_{ph}} + \frac{m_{yx}}{\dot{L}/\dot{V}} \frac{u_L}{\beta_L a_{ph}} \quad (5)$$

$$\beta_L a_{ph} = C_L 12^{1/6} \bar{u}_L^{1/2} \left(\frac{D_L}{d_h} \right)^{1/2} a \left(\frac{a_{ph}}{a} \right) \quad (6)$$

$$\bar{u}_L = \frac{u_L}{h_L} \quad (7)$$

$$\beta_V a_{ph} = C_V \frac{1}{(\varepsilon - h_L)^{1/2}} \frac{a^{3/2}}{d_h^{1/2}} D_V \left(\frac{u_V}{a \nu_V} \right)^{3/4} \left(\frac{\nu_V}{D_V} \right)^{1/3} \left(\frac{a_{ph}}{a} \right) \quad (8)$$

$$\frac{a_{ph}}{a} = 1.5 (a d_h)^{-0.5} \left(\frac{u_L d_h}{\nu_L} \right)^{-0.2} \left(\frac{u_L^2 \rho_L d_h}{\sigma_L} \right)^{0.75} \left(\frac{u_L^2}{g d_h} \right)^{-0.45} \quad (9)$$

$$d_h = 4 \frac{\varepsilon}{a} \quad (10)$$

$$h_L = \left(12 \frac{1}{g} \frac{\eta_L}{\rho_L} u_L a^2 \right)^{1/3} \quad \text{for } u_V \leq u_{V,S} \quad (11)$$

The relations apply to load conditions up to the loading point of a two-phase countercurrent flow, i.e. $u_V \leq u_{V,S}$. Above the loading point, the shear stress of the gas countercurrent is large enough to dam up the falling film so that the column holdup and the size of the interface increase and the effective flow velocity of the falling film decreases. This condition can be taken into account by the equations (12)–(16). For vapour loads less than $u_{V,S}$ the liquid hold-up is according to equation (12) practically $h_{L,S}$.

$$h_L = h_{L,S} + (h_{L,Fl} - h_{L,S}) \left(\frac{u_V}{u_{V,Fl}} \right)^{13} \quad (12)$$

$$h_{L,Fl}^3 (3h_{L,Fl} - \varepsilon) = \frac{6}{g} a^2 \varepsilon \frac{\eta_L}{\rho_L} \frac{L}{V} \frac{\rho_V}{\rho_L} u_{V,Fl} \quad (13)$$

with $\frac{\varepsilon}{3} \leq h_{L,Fl} \leq \varepsilon$

$$\frac{a_{ph}}{a} = \frac{a_{ph,S}}{a} + \left(\frac{a_{ph,Fl}}{a} - \frac{a_{ph,S}}{a} \right) \left(\frac{u_V}{u_{V,Fl}} \right)^{13} \quad (14)$$

$$\frac{a_{ph,Fl}}{a} = 10.5 \left(\frac{\sigma_L}{\sigma_W} \right)^{0.56} (a d_h)^{-0.5} \left(\frac{u_L d_h}{\nu_L} \right)^{-0.2} \left(\frac{u_L^2 \rho_L d_h}{\sigma_L} \right)^{0.75} \times \left(\frac{u_L^2}{g d_h} \right)^{-0.45} \quad (15)$$

$$\bar{u}_L = \left(\frac{g \rho_V^2 u_V^2}{12 \eta_L a^2 \rho_L} \right)^{1/3} \left(\frac{L}{V} \right)^{2/3} \left[1 - \left(\frac{u_V - u_{V,S}}{u_{V,Fl} - u_{V,S}} \right)^2 \right] \quad (16)$$

for $u_{V,S} \leq u_V \leq u_{V,Fl}$

These relations reflect well the results of the experiments if the surface tension along the rectifying column does not change or if it increases. These systems are termed neutral or positive.

In the case of rectification of negative systems, however, which are characterized by the fact that the surface tension

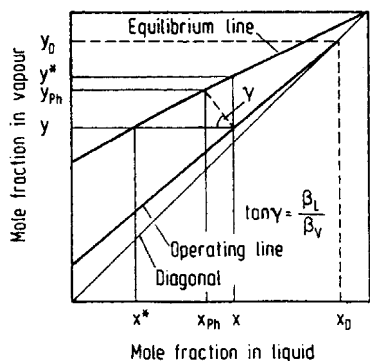


Figure 1. y - x -concentration diagram to describe the overall concentration difference ($x - x^*$) from equilibrium- and operating lines for determination of the Marangoni number.

along the column decreases from the top to the bottom, the Marangoni effect must be taken into account, since additional surface turbulences in the liquid-phase boundary layer reduce the size of the gas-liquid interface. This is taken into account by the Marangoni number according to equation (17) and the interface of negative systems is determined by equation (20). The first term of the Marangoni number describes the change in the surface tension with the concentration along the column while the expression $x - x^*$ takes into account the fictitious concentration difference shifted into the liquid-phase boundary layer, see Figure 1. The liquid-phase mass transfer resistance HTU_L/HTU_{OL} can be calculated by means of equations (18) and (19).

$$Ma_L = \frac{d\sigma_L}{dx} \frac{x - x^*}{D_L \eta_L a} \frac{HTU_L}{HTU_{OL}} \quad (17)$$

$$\frac{HTU_L}{HTU_{OL}} = \frac{X}{1 + X} \quad (18)$$

$$X = \frac{C_V}{C_L} m_{yx} \frac{M_L \rho_V}{M_V \rho_L} \frac{v_L^{1/6}}{v_V^{5/12}} \frac{D_V^{2/3}}{D_L^{1/2}} \frac{a^{1/12}}{g^{1/6} (\epsilon - h_L)^{1/2}} \frac{1}{(\bar{u}_L h_L)^{1/3}} \frac{u_V^{3/4}}{(\bar{u}_L h_L)^{1/3}} \quad (19)$$

$$\left(\frac{a_{ph}}{a} \right)_{neg.Sys.} = \left(\frac{a_{ph}}{a} \right)_{Eq.(6)} (1 - 2.4 \times 10^{-4} |Ma_L|^{0.5}) \quad (20)$$

In the case of extremely large liquid loads, the thickness of the liquid film increases to such large values that voids of the dumped packings or arranged packings are filled up with liquid. The column then operates in a fluid-dynamic range in which the liquid flows as a continuous phase while the gas phase bubbles in a disperse form through the liquid layer. The limiting load, at which one reaches this load range, is termed the inversion point and can be calculated according to extensive studies by means of equation (21). The mass transfer at such high column loads can still be calculated according to the above equations if the liquid load is determined according to equation (22), see Figure 2.

$$\frac{L}{V} \sqrt{\frac{\rho_V}{\rho_L}} = 0.4 \quad \text{for } u_L > 80 \text{ m}^3 \text{ m}^{-2} \text{ h}^{-1} \quad (21)$$

$$u_L = \bar{u}_L h_L = 0.4 u_V \sqrt{\frac{\rho_V}{\rho_L}} \quad (22)$$

Only recently, mass transfer measurements at high pressures

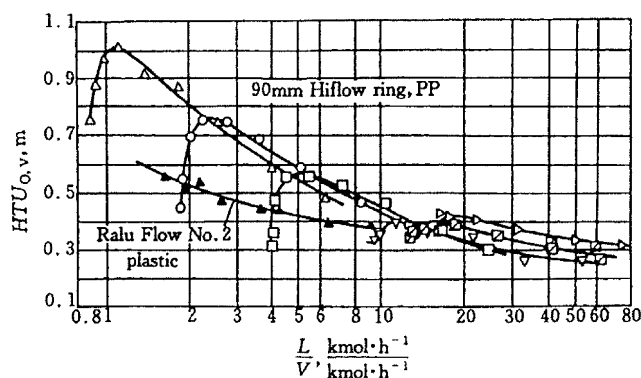


Figure 2. Overall height of a transfer unit $HTU_{O,V}$ as function of the liquid-gas molar flow ratio for Ralu-Flow rings and Hiflow rings at various liquid loads u_L (ammonia-air/water, 293 K, 10^5 Pa).

were included in the experimental database. The comparison with the calculation approaches showed that the extremely low surface tension of the liquid phase at high pressures leads to a large calculated interface for mass transfer. If, however, one takes into account the experimentally confirmed fact that, below a lower limit for the surface tension of 0.03 kg s^{-2} , the surface of metals, plastics or ceramic is completely wet, the influence of the surface tension on the wettability of dumped or arranged packings is lost. This was confirmed by the measurements at high pressures of up to 30 bar. The results of the measurements agreed with the calculated results well if a minimum value of 0.03 kg s^{-2} is used for the surface tension in equations (9) and (15), see Figure 3. The deviations of the calculation to the experimental results are shown in Table 3.

CALCULATION OF THE PRESSURE DROP

On the basis of the theoretical model already mentioned, the pressure drop of an untrickled packing can also be precalculated according to equation (23). It is dependent on the geometric surface and the void volume of the column packings, the gas load factor $F_V = u_V \sqrt{\rho_V}$ which is calculated from the gas velocity and the square root of the gas density and the wall factor K which, according to equation (24), takes into account the increased void fraction at the column wall. The resistance coefficient ψ_0 , see equation (25), is dependent on the Reynolds number Re_V of the gas stream, which depends, in accordance with equation (26), on the particle diameter d_p , see equation (27), and the variables mentioned above.

$$\frac{\Delta p_0}{H} = \psi_0 \frac{a}{\epsilon^3} \frac{F_V^2}{2K} \quad (23)$$

$$\frac{1}{K} = 1 + \frac{2}{3} \frac{1}{1 - \epsilon} \frac{d_p}{d_s} \quad (24)$$

$$\psi_0 = C_{p,0} \left(\frac{64}{Re_V} + \frac{1.8}{Re_V^{0.08}} \right) \quad (25)$$

$$Re_V = \frac{u_V d_p}{(1 - \epsilon) \nu_V} K \quad (26)$$

$$d_p = 6 \frac{1 - \epsilon}{a} \quad (27)$$

Table 2a. Characteristic data and constants for dumped packings.

Dumped Packings		Size mm	N 1 m^{-3}	a $\text{m}^2\text{ m}^{-3}$	ε $\text{m}^3\text{ m}^{-3}$	C_S	C_{FI}	C_h	$C_{P,0}$	C_L	C_V
Raschig Super-Ring	Metal	0.3	180000	315	0.960	3.560	2.340	0.750	0.760	1.500	0.450
		0.5	145000	250	0.975	3.350	2.200	0.620	0.780	1.450	0.430
		1	32000	160	0.980	3.491	2.200	0.750	0.500	1.290	0.440
		2	9500	97.6	0.985	3.326	2.096	0.720	0.464	1.323	0.400
		3	4300	80	0.982	3.260	2.100	0.620	0.430	0.850	0.300
	Plastic	2	9000	100	0.960	3.326	2.096	0.720	0.377	1.250	0.337
Ralu Flow	Plastic	1	33000	165	0.940	3.612	2.401	0.640	0.485	1.486	0.360
		2	4600	100	0.945	3.412	2.174	0.640	0.350	1.270	0.320
Pall ring	Metal	50	6242	112.6	0.951	2.725	1.580	0.784	0.763	1.192	0.410
		35	19517	139.4	0.965	2.629	1.679	0.644	0.967	1.012	0.341
		25	53900	223.5	0.954	2.627	2.083	0.719	0.957	1.440	0.336
	Plastic	50	6765	111.1	0.919	2.816	1.757	0.593	0.698	1.239	0.368
		35	17000	151.1	0.906	2.654	1.742	0.718	0.927	0.856	0.380
		25	52300	225.0	0.887	2.696	2.064	0.528	0.865	0.905	0.446
Ralu ring	Metal	50	6300	105	0.975	2.725	1.580	0.784	0.763	1.192	0.345
		38	14500	135	0.965	2.629	1.679	0.644	1.003	1.277	0.341
		25	51000	215	0.960	2.627	2.083	0.714	0.957	1.440	0.336
	Plastic	50	5770	95.2	0.983	2.843	1.812	0.640	0.468	1.520	0.303
		38	13500	150	0.930	2.843	1.812	0.640	0.672	1.320	0.333
		25	36000	190	0.940	2.841	1.989	0.719	0.800	1.320	0.333
NOR PAC ring	Plastic	50	7330	86.8	0.947	2.959	1.786	0.651	0.350	1.080	0.322
		35	17450	141.8	0.944	3.179	2.242	0.587	0.371	0.756	0.425
		25 ⁶	50000	202.0	0.953	3.277	2.472	0.601	0.397	0.883	0.366
		25 ¹⁰	48920	197.9	0.920	2.865	2.083		0.383	0.976	0.410
Hiflow-ring	Metal	50	5000	92.3	0.977	2.702	1.626	0.876	0.421	1.168	0.408
		25	40790	202.9	0.962	2.918	2.177	0.799	0.689	1.641	0.402
		50	6815	117.1	0.925	2.894	1.871	1.038	0.327	1.478	0.345
	Plastic	50 hydr.	6890	118.4	0.925	2.894	1.871		0.311	1.553	0.369
		50 S	6050	82.0	0.942	2.866	1.702	0.881	0.414	1.219	0.342
		25	46100	194.5	0.918	2.841	1.989		0.741	1.577	0.390
	Ceramic	50	5120	89.7	0.809	2.819	1.694		0.538	1.377	0.379
		38	13241	111.8	0.788	2.840	1.930		0.621	1.659	0.464
		20	121314	286.2	0.758	2.875	2.410	1.167	0.628	1.744	0.465
Glitsch ring	Metal	30 PMK	29200	180.5	0.975	2.694	1.900	0.930	0.851	1.920	0.450
		30 P	31100	164.0	0.959	2.564	1.760	0.851	1.056	1.577	0.398
Glitsch CMR ring	Metal	1.5"	60744	174.9	0.974	2.697	1.841	0.935	0.632		
		1.5" T	63547	188.0	0.972	2.790	1.870	0.870	0.627		
		1.0"	158467	232.5	0.971	2.703	1.996	1.040	0.641		
		0.5"	560811	356.0	0.952	2.644	2.178		0.882	2.038	0.495
TOP Pak ring	Alu	50	6871	105.5	0.956	2.528	1.579	0.881	0.604	1.326	0.389
Raschig ring	Ceramic	50	5990	95.0	0.830	2.482	1.547			1.416	0.210
		25	47700	190.0	0.680	2.454	1.899	0.577	1.329	1.361	0.412
VSP ring	Metal	50	7841	104.6	0.980	2.806	1.689	1.135	0.773	1.222	0.420
		25	33434	199.6	0.975	2.755	1.970	1.369	0.782	1.376	0.405
Envi Pac ring	Plastic	80	2000	60.0	0.955	2.846	1.522	0.641	0.358	1.603	0.257
		60	6800	98.4	0.961	2.987	1.864	0.794	0.338	1.522	0.296
		32	53000	138.9	0.936	2.944	2.012	1.039	0.549	1.517	0.459
Bialecki ring	Metal	50	6278	121.0	0.966	2.916	1.896	0.798	0.719	1.721	0.302
		35	18200	155.0	0.967	2.753	1.885	0.787	1.011	1.412	0.390
		25	48533	210.0	0.956	2.521	1.856	0.692	0.891	1.461	0.331
Tellerette	Plastic	25	37037	190.0	0.930	2.913	2.132	0.588	0.538	0.899	
Hackette	Plastic	45	12000	139.5	0.928	2.832	1.966	0.643	0.399		
Raflux ring	Plastic	15	193522	307.9	0.894	2.825	2.400	0.491	0.595	1.913	0.370
Berl saddle	Ceramic	25	80080	260.0	0.680			0.620		1.246	0.387
		13	691505	545.0	0.650			0.833		1.364	0.232
DIN-PAK	Plastic	70	9763	110.7	0.938	2.970	1.912	0.991	0.378	1.527	0.326
		47	28168	131.2	0.923	2.929	1.991	1.173	0.514	1.690	0.354

Table 2b. Characteristic data and constants for regular packings.

Dumped Packings		Size mm	N 1 m^{-3}	a $\text{m}^2\text{ m}^{-3}$	ε $\text{m}^3\text{ m}^{-3}$	C_S	C_{FI}	C_h	$C_{P,0}$	C_L	C_V
Pall ring	Ceramic	50	7502	155.2	0.754	3.793	3.024	1.066	0.233	1.278	0.333
Bialecki ring	Metal	35	20736	176.6	0.945			0.690	0.460	1.405	0.377
Ralu pak	Metal	YC-250		250.0	0.945	3.178	2.558		0.191	1.334	0.385
Mellapak	Metal	250Y		250.0	0.970	3.157	2.464	0.554	0.292		
Gempack	Metal	A2T-304		202.0	0.977	2.986	2.099	0.678	0.344		
Impulse packing	Metal	250		250.0	0.975	2.610	1.996	0.431	0.262	0.983	0.270
	Ceramic	100		91.4	0.838	2.664	1.655	1.900	0.417	1.317	0.327
Montz packing	Metal	B1-200		200.0	0.979	3.116	2.339	0.547	0.355	0.971	0.390
		B2-300		300.0	0.930	3.098	2.464	0.482	0.295	1.165	0.422
	Plastic	C1-200		200.0	0.954				0.453	1.006	0.412
		C2-200		200.0	0.900	2.653	1.973		0.481	0.739	
Euroform	Plastic	PN-110		110.0	0.936	3.075	1.975	0.511	0.250	0.973	0.167

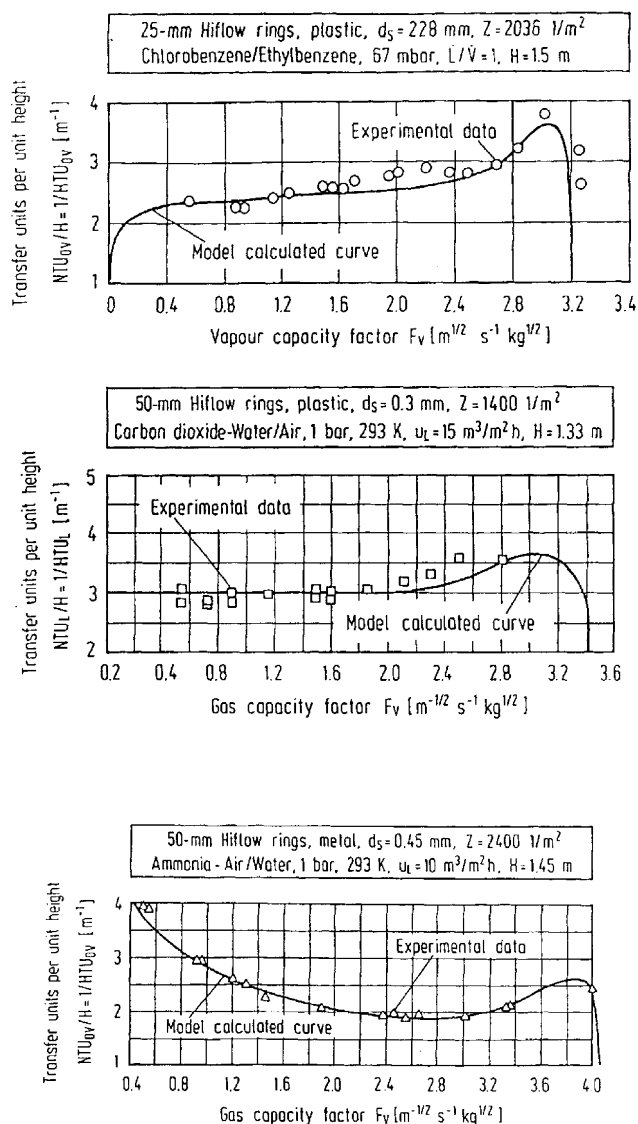


Figure 3. Comparison of the load-efficiency relationship calculated from the model correlations with that determined in rectification, absorption and desorption experiments.

When dumped packings or arranged packings are irrigated, the free cross-section for the gas flow is reduced by the column holdup, and the surface structure is changed as the result of the coating with the liquid film. Thus the column holdup h_L according to equation (11) must be taken into account by equation (28) and the resistance coefficient of the two-phase flow ψ_L defined by equation (29). It is dependent on the Froude number of the flow of liquid and on

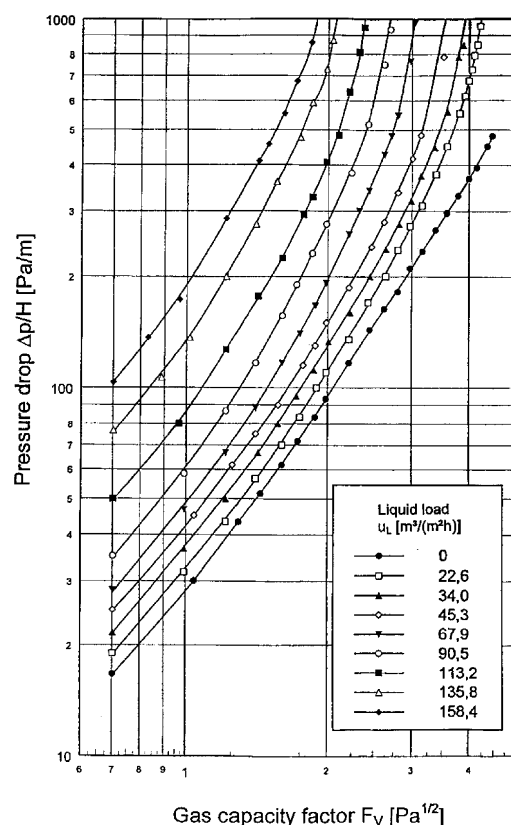


Figure 4. Pressure drop diagram of Raschig Super-Ring No. 2, metal. Test system: water/air; Number of driplet points: 951 l m^{-2} ; Packing height: $H = 3.0$ m; Temperature of gas: $T = 6^\circ\text{C}$; Column diameter: $d = 0.75$ m; Operating pressure: 1 bar; Specific surface area: $a = 98\text{ m}^2\text{ m}^{-3}$; Void fraction: $\varepsilon = 0.98\text{ m}^3\text{ m}^{-3}$.

Table 3. Average relative deviations for calculating loading and flooding point, holdup, pressure drop and mass transfer efficiency with the model equations.

Loading and flooding point	Column holdup h_L	Pressure drop $\Delta p/H$	Mass transfer efficiency	
			Absorption and Desorption	Rectification
5%	6,7%	9,1%	12,4%	14,1%

the liquid holdup. The packing-specific constant $C_{P,0}$ can be found in Table 2. This relation applies throughout the load range of a mass transfer column, i.e. up to the flooding point of the two-phase countercurrent flow, see Figure 4.

$$\frac{\Delta p}{H} = \psi_L \frac{a}{(\varepsilon - h_L)^3} \frac{F_V^2}{2K} \quad (28)$$

$$\psi_L = C_{P,0} \left(\frac{64}{Re_V} + \frac{1.8}{Re_V^{0.08}} \right) \left(\frac{\varepsilon - h_L}{\varepsilon} \right)^{1.5} \left(\frac{h_L}{h_{L,S}} \right)^{0.3} \times \exp \left(C_1 \sqrt{Fr_L} \right) \quad \text{with } C_1 = \frac{13300}{a^{3/2}} \quad (29)$$

$$Fr_L = \frac{u_L^2 a}{g} \quad (30)$$

In the previous publications by Billet and Schultes, the dependency of the resistance coefficient ψ_L on the liquid load u_L was expressed by the Reynolds number in the exponential function of equation (29). The measurements at high pressures already mentioned and at extremely low liquid viscosities, however, showed with reference to the pressure drops that such systems can be taken into account better in the pressure drop calculation if, instead of the Reynolds number, the Froude number describes the dependency on the liquid load, see equation (30). The deviations of the calculation to the experimental results are shown in Table 3.

CALCULATION OF THE LOAD LIMITS

The above explanations show clearly that the loading point and the flooding point represent two characteristic load conditions of dumped- or arranged-type packed columns. Below the loading point, the liquid film trickles from the top of the column to the bottom of the column, not influenced by the gas countercurrent flow. The column holdup is then merely a function of the liquid load. With increasing gas velocity, the shearing stress at the surface of the liquid increases so that the velocity of the liquid film at the phase-boundary layer drops. At the loading point, the velocity at the interface is zero, and thus the calculation equation for the loading point is derived according to equation (31).

The resistance coefficient at the loading point ψ_s is determined by means of equation (32) and is dependent on the L/V mass flow ratio. The latter also links the phase velocities to the loading point in accordance with equation (33) so that the relations for a given L/V ratio can only be solved by iteration. The exponent n_s is dependent according to equations (34) and (35) on the given flow parameter which characterizes the load condition for the phase inversion in the column. If the flow parameter is smaller than 0.4, the liquid trickles downwards over the internals towards the gas flow as a disperse phase, while if the flow parameter is greater than 0.4, the liquid load and thus the column holdup reach such large values that the empty

spaces within the bed close up and the liquid flows downwards as a continuous phase. The gas phase then rises up through the liquid layer in the form of bubbles. The packing-specific constant C_s can be found in Table 2.

$$u_{V,S} = \sqrt{\frac{g}{\psi_s} \left[\frac{\varepsilon}{a^{1/6}} - a^{1/2} \left(12 \frac{1}{g} \frac{\eta_L}{\rho_L} u_{L,S} \right)^{1/3} \right]} \times \left(12 \frac{1}{g} \frac{\eta_L}{\rho_L} u_{L,S} \right)^{1/6} \sqrt{\frac{\rho_L}{\rho_V}} \quad (31)$$

$$\psi_s = \frac{g}{C_s^2} \left[\frac{L}{V} \sqrt{\frac{\rho_V}{\rho_L} \left(\frac{\eta_L}{\eta_V} \right)^{0.4}} \right]^{-2n_s} \quad (32)$$

$$u_{L,S} = \frac{\rho_V}{\rho_L} \frac{L}{V} u_{V,S} \quad (33)$$

$$\text{for } \frac{L}{V} \sqrt{\frac{\rho_V}{\rho_L}} \leq 0.4 : n_s = -0.326; C_s \text{ from Table 2} \quad (34)$$

$$\text{for } \frac{L}{V} \sqrt{\frac{\rho_V}{\rho_L}} \geq 0.4 : n_s = -0.723; C_s = 0.695 C_{s,Tab.2} \left(\frac{\eta_L}{\eta_V} \right)^{0.1588} \quad (35)$$

If the gas velocity rises above the loading point, the flow of liquid is impeded and the column holdup increases. If the shear stress of the gas counterflow is sufficient to entrain the entire liquid to the top of the column, then the flooding point of the mass transfer column is reached. This means mathematically that the velocity gradient of the liquid film becomes zero at the interface to the dumped packing. equations (36)–(40) can be derived from this condition for the calculation of the flooding point of dumped- and arranged-type columns.

$$u_{V,FI} = \sqrt{2} \sqrt{\frac{g}{\psi_{FI}} \frac{(\varepsilon - h_{L,FI})^{3/2}}{\varepsilon^{1/2}}} \sqrt{\frac{h_{L,FI}}{a}} \sqrt{\frac{\rho_L}{\rho_V}} \quad (36)$$

$$\psi_{FI} = \frac{g}{C_{FI}^2} \left[\frac{L}{V} \sqrt{\frac{\rho_V}{\rho_L} \left(\frac{\eta_L}{\eta_V} \right)^{0.2}} \right]^{-2n_{FI}} \quad (37)$$

$$u_{L,FI} = \frac{\rho_V}{\rho_L} \frac{L}{V} u_{V,FI} \quad (38)$$

$$\text{for } \frac{L}{V} \sqrt{\frac{\rho_V}{\rho_L}} \leq 0.4 : n_{FI} = -0.194; C_{FI} \text{ from Table 2} \quad (39)$$

$$\text{for } \frac{L}{V} \sqrt{\frac{\rho_V}{\rho_L}} \geq 0.4 : n_{FI} = -0.708; C_{FI} = 0.6244 C_{FI,Tab.2} \left(\frac{\eta_L}{\eta_V} \right)^{0.1028} \quad (40)$$

The column holdup at the flooding point, which is to be substituted in equation (36), is calculated from equation (13). The constants C_{FL} can be found in Table 2.

The design of dumped- and arranged-type columns generally takes place for column loads of 70–80% of the flooding load. Above the loading point, which is at about 70% of the flooding load, the mass transfer efficiency initially increases, since the interface becomes larger. In the vicinity of the flooding point the efficiency of the column packings, however, drops again drastically since the back mixing in the liquid phase increases in such a way that the positive effect of the enlarged interface is overcompensated. Furthermore, the pressure drop in the vicinity of the flooding point becomes extremely high. Therefore, the operation of absorption, desorption and rectification columns with loads over 80% of the flooding load is uneconomical. The deviations of the calculation to the experimental results are shown in Table 3.

CALCULATION OF THE REAL COLUMN HOLDUP

The column holdup used in the calculation approaches above resulted from the physical model which approximates the void volume of dumped packings or of an arranged packing by vertical, parallel flow channels. A real dumped- or arranged-type packing consists of flow channels through which the phases flow only with permanent changes in direction and whose surface often is only partly covered by the liquid. As a result of this, the theoretical column holdup substituted in the previous relations deviates from the real column holdup.

Numerous measurements on the column holdup with different systems document that the deviation between the theoretical and the real column holdup can be expressed by means of a hydraulic surface area of the packing. The real column holdup can be described by equation (41) as a function of the liquid load and the previously mentioned material properties and the hydraulic surface area a_h . Equations (42) and (43) show that the hydraulic surface area increases less in the range of low Reynolds numbers than with large Reynolds numbers, if the liquid load becomes higher.

$$h_L = \left(12 \frac{1}{g} \frac{\eta_L}{\rho_L} u_L a^2 \right)^{1/3} \left(\frac{a_h}{a} \right)^{2/3} \quad (41)$$

$$Re_L = \frac{u_L \rho_L}{a \eta_L} < 5 : \frac{a_h}{a} = C_h \left(\frac{u_L \rho_L}{a \eta_L} \right)^{0.15} \left(\frac{u_L^2 a}{g} \right)^{0.1} \quad (42)$$

$$Re_L = \frac{u_L \rho_L}{a \eta_L} \geq 5 : \frac{a_h}{a} = C_h 0.85 \left(\frac{u_L \rho_L}{a \eta_L} \right)^{0.25} \left(\frac{u_L^2 a}{g} \right)^{0.1} \quad (43)$$

$$h_{L,FI} = 2.2 h_L \left(\frac{\eta_L \rho_W}{\eta_W \rho_L} \right)^{0.05} \quad (44)$$

The prediction of the real column holdup above the loading point is made by using equation (12) with the column holdup $h_{L,S}$ calculated by equation (41) and $h_{L,FI}$ calculated by equation (44).

The averages of the absolute deviations of the calculated values from the experimental results are shown in Table 3.

NOMENCLATURE

a	specified surface area of the dumped packing, $\text{m}^2 \text{m}^{-3}$
C	constant

d	diameter, m
D	diffusion coefficient, $\text{m}^2 \text{s}^{-1}$
F_v	gas or vapour capacity factor, $\sqrt{\text{Pa}}$
g	gravitational acceleration, m s^{-2}
H	height, m
HTU	height of a transfer unit, m
h_L	column holdup, $\text{m}^3 \text{m}^{-3}$
K	wall factor
K_o	overall mass transfer coefficient
L	mass flow of the liquid, kg h^{-1}
\dot{L}	molar flow of the liquid, kmol h^{-1}
M	molecular weight, kg kmol^{-1}
m_{ex}	slope of the equilibrium curve, kmol kmol^{-1}
N	packing density 1, m^{-3}
NTU	number of transfer units
n	exponent
Δp	pressure drop, Pa
u	velocity with reference to the free column cross-section, $\text{m}^3 \text{m}^{-2}$
\bar{u}	mean effective velocity, m s^{-1}
V	mass flow of the gas or vapour, kg h^{-1}
\dot{V}	molar flow of the gas or vapour, kmol h^{-1}
x	molar concentration in the liquid, kmol h^{-1}

Greek letters

β	mass transfer coefficient, m s^{-1}
ε	void fraction, $\text{m}^3 \text{m}^{-3}$
η	dynamic viscosity, kg ms^{-1}
λ	stripping factor
ν	kinematic viscosity, $\text{m}^2 \text{s}^{-1}$
ρ	density, kg m^{-3}
σ	surface tension, kg s^{-2}
ψ	resistance coefficient

Indices

FI	flooding point
h	hydraulic
L	liquid
O	total
P	particles
Ph	interface
S	loading point
S	column
V	gas or vapour
W	water

REFERENCES

1. Billet, R., 1983, *Festschrift* [commemorative publication] (Fakultät für Maschinenbau, Ruhr-Universität Bochum), p. 24–31.
2. Billet, R., 1987, *ICHEME Symp Ser No. 104*, p. A171–A182.
3. Billet, R. and Schultes, M., 1987, *ICHEME Symp Ser No. 104*, p. B255–B266.
4. Billet, R. and Schultes, M., 1991, In *Beiträge zur Verfahrens- und Umwelttechnik*, (Ruhr-Universität Bochum), p. 88–107 and 108–122.
5. Billet, R. and Schultes, M., 1991, *Chem Eng Technol*, 14: 89–95.
6. Billet, R. and Schultes, M., 1992, *ICHEME Symp Ser No. 128*, p. B129–B139.
7. Schultes, M., 1990, *Doctoral dissertation*, (Ruhr-Universität Bochum, Fortschritt-Berichte VDI Series 3 No. 230, VDI-Verlag, Düsseldorf).
8. Billet, R., 1992, *Chem-Ing-Technol*, 64: 401–410.
9. Billet, R. and Schultes, M., 1993, *Chem Eng Technol*, 16: 1–9.
10. Billet, R. and Schultes, M., 1993, *Chem Eng Technol*, 16: 370–375.
11. Billet, R. and Schultes, M., 1995, *Chem Eng Technol*, 18: 371–379.
12. Billet, R., 1995, *Packed Towers in Processing and Environmental Technology*, (VCH).

ADDRESS

Correspondence concerning this paper should be addressed to Dr.-Ing. M. Schultes, Raschig GmbH, Mundenheimers trasse 100, D-67061 Ludwigshafen, Germany.

The manuscript was received 11 February 1999 and accepted for publication after revision 10 June 1999.